NASA TN D-384

TECHNICAL NOTE
D-384

COMBINATIONS OF SHEAR, COMPRESSIVE THERMAL, AND COMPRESSIVE LOAD STRESSES FOR THE ONSET OF PERMANENT BUCKLES IN PLATES

By George W. Zender and John B. Hall, Jr.

Langley Research Center
Langley Field, Va.

NATIONAL AERONAUTICS AND SPACE ADMINISTRATION
WASHINGTON
May 1960

NATIONAL AERONAUTICS AND SPACE ADMINISTRATION

TECHNICAL NOTE D-384

COMBINATIONS OF SHEAR, COMPRESSIVE THERMAL, AND COMPRESSIVE LOAD STRESSES FOR THE ONSET OF PERMANENT BUCKLES IN PLATES

By George W. Zender and John B. Hall, Jr.

SUMMARY

A semiempirical method of evaluating the onset of permanent buckles in plates in the presence of combinations of shear, thermal compressive, and compressive load stresses is given. It is shown that the shear and compressive stresses required for the onset of permanent buckles may be approximated by a parabolic interaction curve. Thermal stresses are included by treating the compressive stress as being composed of a thermal component and a load component and employing the appropriate material properties at the elevated temperature. The results show that the compressive load stress which a plate can support at the onset of permanent buckles is reduced by thermal compressive stresses and by shear stresses. Results of the method are compared with experimental values for the onset of permanent buckles obtained from tests of square tubes of 17-7 PH (Condition TH 1050) stainless steel.

INTRODUCTION

The thermal stresses in the structure of high-speed aircraft or missiles in combination with stresses due to air loads may produce severe buckling of the thin skin surfaces. The integrity of the structure may remain after considerable skin buckling; however, buckles may become permanent and cause considerable concern. Unfortunately, very little information is available on the conditions which cause permanent buckles.

In 1941, Howland and Sandorff (ref. 1) investigated permanent buckles at room temperatures in alclad 24S-T (now designated 2024-T) aluminum-alloy sheet-stringer panels loaded in compression and developed a method of analysis which is applicable to aircraft design. Basically, the method associates permanent buckles with the extreme fiber strain on the concave side of the buckle crest. Until this particular strain at the surface of the plate becomes plastic, permanent buckles are not expected to occur.

However, as noted in reference 1, surface irregularities develop in the construction of aircraft so that permanent buckles actually exist to some extent before aerodynamic loads are introduced. In order to circumvent this practical consideration, permanent buckles of sufficient magnitude to be "objectionable" were defined. For objectionable permanent buckles to occur, it is necessary that the particular reference strain at the surface of the plate progress well into the plastic range where the stress-strain relations of plates are not given by simple equations and solutions for even the simplest loading cases are obtained only with considerable difficulty. (See ref. 2.) Also, as mentioned in reference 1, strains even larger than the extreme fiber strain at the concave side of the buckle crest may exist in buckled plates.

In view of the difficulties inherent in associating permanent buckling with a particular extreme fiber strain at a point on a plate, recent studies at the Langley Research Center have attempted to associate permanent buckles with a quantity expressing overall action of the fibers in a plate. For compressive loads, such an overall action is indicated by the unit shortening of the plate and this approach was employed in reference 3 to evaluate the combinations of compressive thermal and compressive load stresses for the onset of permanent buckles in plates. The present paper extends the results presented in reference 3 to include shear stresses so that the onset of permanent buckles in plates may be approximated for shear stresses, compressive load or compressive thermal stresses, or combinations of these stresses. Also included are the results of tests performed on 17-7 PH (Condition TH 1050) stainless-steel square tubes to obtain experimental values for the onset of permanent buckles.

SYMBOLS

A	cross-sectional area, sq in.
b	width, in.
E	modulus of elasticity at average temperature of skin or web, ksi
e	unit shortening or extension
m	exponent used in equation (1)
R	stress ratio
T	temperature, $^{\circ}F$
$\overline{T}$	temperature rise from initial temperature, $^{\circ}F$

t thickness, in.

α average coefficient of thermal expansion for particular temperature range, per ^{o}F

$$\beta = \frac{\epsilon_{cr}}{2}\left(\frac{E_s A_s}{E_w A_w}\right)^2$$

γ shear strain

ϵ strain

η plasticity factor

θ angle of twist, radians

μ Poisson's ratio

σ stress

$\overline{\sigma}$ average stress

τ shear stress

$\overline{\tau}$ average shear stress

Subscripts:

cr critical (classical or initial buckling of skin)

e edge

eff effective

el elastic limit

f failure

pb permanent buckling

s skin

w web or stringer

Superscripts:

C compression

L load

S shear

T thermal

METHOD OF ANALYSIS AND RESULTS

In this section a semiempirical method for evaluating the onset of permanent buckles of plates in the presence of shear, compressive load, and thermal compressive stresses or combinations of these stresses is developed. Compressive stresses are considered initially, and then pure shear stresses are discussed. Combined compressive and shear stresses are next considered and, finally, a method is given for including thermal stresses with compressive, shear, or combined compressive and shear stresses. Experimental results described in the appendixes are presented along with the development of the method of analysis.

L 3 3 4

Onset of Permanent Buckles for Compressive Stresses

In the course of compressive testing of skin-stringer panels it has been observed that permanent buckles of the skin of the panels, when the skin buckles elastically, usually occur when the unit shortening of the panel is in the vicinity of the elastic limit strain of the skin material; for panels in which skin buckling occurs beyond the elastic range, permanent buckles occur essentially when the skin buckles. Some indication of the validity of this observation is shown in figure 1 in which the approximation is compared with experimental data obtained from reference 1. The squares in figure 1 represent compressive test data at room temperature for alclad 24S-T (now 2024-T) skin-stiffened panels. The edge stress σ_e, when objectionable permanent buckles (permanent-buckle depth or twice wave amplitude = $0.00027b/t$) occur in the skin, is given as a function of the skin buckling stress. The parameters in figure 1 are given in nondimensional form in order to include data from the tests described in appendix A for the onset of permanent buckles in square tubes made of 17-7 PH (Condition TH 1050) stainless steel. The horizontal line in figure 1 represents the elastic limit stress and the inclined line represents the edge or stiffener stresses equal to the buckling stress. Only the solid portion of the inclined line, which represents stresses beyond the elastic limit stress, is of interest herein. Substantial agreement between the approximation and the experimental results is indicated in figure 1 although some concern exists regarding the two test points which fall below the horizontal line. Since the test data shown by the square symbols represent objectionable

permanent buckles rather than the onset of permanent buckles, these square symbols would be expected to lie slightly above the horizontal and inclined solid lines.

The information shown in figure 1 deals with the edge or stiffener stress. The average stress on a plate for the onset of permanent buckles may be approximated from an average-stress—unit-shortening relation of the type given by equation (C1) of reference 4, as follows:

$$\frac{\bar{\sigma}}{\sigma_e} = \left(\frac{\epsilon_{cr}}{e_e}\right)^{1-m} \tag{1}$$

The exponent 1-m for simply supported plates is often taken as 1/2 and with this value the average stress for the onset of permanent buckles may be written for $\sigma_e = \sigma_{el}$ as

$$\bar{\sigma}_{pb} = \sqrt{\sigma_{cr}\sigma_{el}} \qquad \left(\sigma_{cr} < \sigma_{el}\right) \tag{2}$$

This relation is shown in figure 2 along with the test data for stainless-steel square tubes given in table 1 for the case of pure compression. The average stress on the plate at the onset of permanent buckles is shown as a function of the buckling stress. Beyond the elastic limit stress the stress for the onset of permanent buckles is taken as equal to the buckling stress indicated by the straight line on the upper portion of figure 2.

On the basis of the information presented in figures 1 and 2, it is assumed that the onset of permanent buckles in simply supported plates loaded in compression occurs approximately when the unit shortening of the plate is equal to the elastic limit strain for plates which buckle elastically; for plates which buckle beyond the elastic range, the onset of permanent buckles occurs essentially at plate buckling.

Onset of Permanent Buckles for Shear Stresses

In order to obtain experimental information regarding permanent buckles in shear, twisting tests were performed on square tubes as described in appendix A. The results are shown in figure 3 in a form similar to that of figure 1 except that shear stresses rather than compressive stresses are now involved. The horizontal line represents the

shear elastic limit stress obtained from the compressive and tensile stress-strain curves by the method of reference 5 and the inclined line represents the shear stresses equal to the buckling stress. The results indicate that the approximation for the onset of permanent buckles for compressive loads may also be applicable for shear stresses.

The average shear stresses for the onset of permanent buckling of the square tubes subjected to torque are shown as a function of the shear buckling stress by the symbols in figure 4. The curve in the figure (see table 2 calculations) was obtained from an equation of the same form as that given previously for compression - namely,

$$\bar{\tau}_{pb} = \sqrt{\tau_{cr}\tau_{el}} \qquad (\tau_{cr} < \tau_{el}) \qquad (3)$$

For buckling stresses beyond the elastic range, the shear stress for the onset of permanent buckling was taken as equal to the buckling stress as given by the straight line in figure 4. Again the agreement of the experiment and the approximation appears reasonable.

It should be mentioned that the shear stiffness of plates after buckling can be appreciably influenced by longitudinal or transverse stiffening. For such cases equation (3) can be considerably in error. The effect of longitudinal and transverse stiffening of plates on the shear stiffness after buckling is given in reference 6 and the results may be used to modify equation (3) to account for the effect of the stiffening.

On the basis of the information presented in figures 3 and 4, it is assumed that the onset of permanent buckling in simply supported plates loaded in shear occurs approximately when the average shear strain of the plate is equal to the shear elastic limit strain for plates which buckle elastically; for plates which buckle beyond the elastic range, the onset of permanent buckles occurs essentially when the plate buckles.

Onset of Permanent Buckles for Combined Compressive and Shear Stresses

The combined compressive and shear stresses for the onset of permanent buckles in plates may be expressed in interaction-curve form similar to that in which buckling for combined loads is often expressed. In order to find an appropriate expression for the shape of the interaction curve for permanent buckles, tests were performed on square tubes

subjected to compression and shear as described in appendix A. The results are given in table 1 and are also shown in figure 5 where the open test points represent the onset of permanent buckles and the solid test points represent failure. The ordinate and abscissa of figure 5 are experimental stress ratios of the usual type employed for interaction curves. Also shown in the figure is the parabolic expression for elastic buckling due to combined compression and shear. Figure 5 indicates that the parabolic interaction curve expresses with reasonable accuracy the onset of permanent buckles and failure due to combined compression and shear when initial buckling occurs elastically. It should be noted that the results shown in figure 5 involve elastic buckling except for the case of the square tube with $b/t = 40$ for which buckling exceeds the elastic limit only in shear. It is possible that, for plates with plastic buckling in both compression and shear, another expression might be more appropriate for the onset of permanent buckles or failure, such as the circular arc recommended in reference 7 for the case of plastic buckling due to combined compression and shear. For the results presented herein, however, the parabolic expression appears reasonable. The amount of compressive stress for the onset of permanent buckles for a prescribed shear stress, or vice versa, may be calculated from the parabolic expression where the pure stress for the onset of permanent buckling used in the denominators of the stress ratios R^C and R^S are as given by equations (2) and (3), respectively for elastic buckling, or by the critical buckling stresses for the case of plastic buckling. In figure 6 is shown a comparison of the experimental (symbols) and calculated (curves) stresses for the onset of permanent buckles of the square tubes.

Onset of Permanent Buckles for Combinations of Compressive Load, Shear, and Compressive Thermal Stresses

In this section, the approximate method of evaluating the onset of permanent buckles in plates subjected to compression, shear, or combined compression and shear is extended to include the effects of restrained thermal expansion of the plate. The structure treated in this case is shown schematically in figure 7. It consists of a long plate of constant thickness bounded along the side edges by longitudinals of constant cross section. The plate is continuously attached to the longitudinals but is not restrained against edge rotation nor in-plane displacement normal to the longitudinals. In addition to applying compressive, shear, or combined compressive and shear loads, the plate is assumed to be rapidly heated so that it is subjected to a uniform temperature T_s while a lower temperature T_w exists in the longitudinals. Temperatures are limited to the range in which the characteristic shapes of the material stress-strain curves are preserved although the modulus, elastic

limit, and yield stresses may be considerably reduced from the room-temperature values. The thermal condition is assumed to result in a uniform restraint of the free thermal expansion of the plate and correspondingly in a uniform extension in addition to the free thermal expansion of the longitudinals. The compressive stress and unit shortening in the plate due to the restrained thermal expansion is evaluated in appendix B. The thermal compressive unit shortening is added to the compressive unit shortening due to load which results in a total compressive unit shortening in the plate. For compressive load and thermal stress, the onset of permanent buckles when buckling occurs elastically is presumed to occur when this total compressive unit shortening in the plate exceeds the elastic limit strain of the material at the temperature of the plate (ref. 3). For shear load and thermal stress, the onset of permanent buckles is presumed to be given by the parabolic interaction curve where the compressive stress is that due to the restrained thermal expansion on the plate. Similarly, for combined compressive load, compressive thermal, and shear stress the onset of permanent buckles is presumed to be given by the parabolic interaction curve where the compressive stress is the total of the compressive load stress and compressive thermal stress. The validity of the parabolic assumption for the combined stress conditions was obtained from tests of six square tubes as described in appendix C. The results of the tests for the heated sides of the tubes are shown as stress ratios for the onset of permanent buckles in figure 8. The portion of the total compressive stress due to thermal stress is indicated by dashed lines with arrowheads and the remainder due to compressive load stress is indicated above the arrowheads by solid lines. Two of the vertical lines are offset in order to avoid confusion with other data in the figure. As indicated in figure 8, a significant portion of the compressive stress is composed of thermal stress which provided a rather severe thermal check of the analysis for the onset of permanent buckles.

CONCLUDING REMARKS

A semiempirical method of evaluating the onset of permanent buckles in plates in the presence of combinations of shear, compressive thermal, and compressive load stresses is given. It is shown that the combined shear and compressive stresses for the onset of permanent buckles may be approximated by parabolic interaction curves of the type used for determining buckling stresses. Thermal stresses may be included in the analysis as a component of the compressive stresses.

The limited amount of test data given indicates that the semiempirical method reasonably predicts the shear, compressive, and thermal stress conditions for the onset of permanent buckles in plates. The presence of shear stresses substantially reduces the amount of compressive stress

which may be applied for the onset of permanent buckles or failure or, conversely, the presence of compressive stresses substantially reduces the amount of shear stress which may be applied. A similar result occurs when the compressive stress is composed of a thermal component as well as a load component.

Langley Research Center,
National Aeronautics and Space Administration,
Langley Field, Va., February 18, 1960.

APPENDIX A

TESTS OF SQUARE TUBES AT ROOM TEMPERATURE

Experimental information on the permanent buckling of plates was obtained from tests of ten square tubes of the type shown in figure 9. Each tube consisted of two formed channels 32 inches in length and 1/16 inch in thickness of 17-7 PH (Condition TH 1050) stainless-steel material. The channels were welded together along the flanges to form square tubes. The midplanes of opposite walls of the tubes were spaced $2\frac{1}{2}$, $3\frac{3}{4}$, or $5\frac{1}{4}$ inches which resulted in width-to-thickness ratios of the walls of 40, 60, and 84, respectively. The tubes were tested at room temperature and were subjected to torsion, compression, or combined torsion and compression in the combined load testing machine of the Langley structures research laboratory. The tubes were loaded slightly beyond buckling and were then unloaded and a survey of the walls which did not contain weld seams was made with a pantograph apparatus to determine the degree of permanent buckling. This procedure was repeated a number of times, with the tubes being subjected to a higher loading each time until failure occurred. (The tubes subjected to combined torsion and compression were subjected to the full torque initially on each loading and the compression load was progressively increased. Similarly, in unloading, the torque was removed last.) Figure 10 shows an example of the type of permanent-buckle information obtained. The permanent-buckle depths shown are the average of the double amplitude of the waves in the two opposite walls of the tube. The lower point is the average of the initial irregularities measured before the tube was subjected to load. The onset of permanent buckles was selected as the point beyond which the initial imperfections in the tubes began to increase, as indicated in figure 10. The shear and compressive stresses at which permanent buckles and failure occurred for each of the tubes are given in table 1.

In addition to the permanent-buckle-depth measurements, the lengthwise unit shortening of the tubes tested in pure compression was obtained from the average of four Baldwin SR-4 type A-9 strain gages located near the corners at the midlength of the tubes; also, the twist of the tubes tested in pure shear was obtained at two spanwise stations, each $10\frac{1}{2}$ inches from the center cross section of the tubes. The difference of the twist measurements $\Delta\theta$ was converted to average shear strain in the walls of the tube by the following relation:

$$\gamma = \frac{\Delta\theta b/2}{21}$$

The unit-shortening values for the tubes tested in pure compression were converted to edge stress by using the compressive stress-strain curve of the material and are shown by the circles in figure 1. For the square tubes subjected to torque, the shear strain was converted to shear stress by using the shear stress-strain curve obtained from the compressive and tensile stress-strain curves by the method of reference 5. These shear stresses are shown by the circles in figure 3.

APPENDIX B

THERMAL COMPRESSIVE STRESS AND UNIT SHORTENING

For unbuckled skin, the compressive unit shortening due to uniform skin and stringer temperatures for the structure shown in figure 7 is from elementary theory

$$e_s{}^T = \frac{\alpha_s \bar{T}_s - \alpha_w \bar{T}_w}{1 + \frac{E_s A_s}{E_w A_w}} \qquad \left(e_s{}^T < \epsilon_{cr} < \epsilon_{el}\right) \tag{B1}$$

and the corresponding stress is simply

$$\sigma_s{}^T = E_s e_s{}^T \tag{B2}$$

When the skin is buckled, the thermal compressive unit shortening in the skin may be approximated by employing the effective-area concept in order to account for the reduced stiffness of the skin. If equation (1) with the exponent $1\text{-}m = \frac{1}{2}$ is taken as the average-stress—unit-shortening relationship of the skin, the effective area of the skin beyond buckling is given by

$$A_{s,eff} = A_s \sqrt{\frac{\epsilon_{cr}}{e_s{}^T}} \tag{B3}$$

Introducing the effective area of the skin into equation (B1) in place of the area A_s yields a quadratic expression for the compressive thermal unit shortening in the skin for which the root of practical significance here is

$$\sqrt{e_s{}^T} = -\sqrt{\frac{\beta}{2}} + \sqrt{\frac{\beta}{2} + \left(\alpha_s \bar{T}_s - \alpha_w \bar{T}_w\right)} \tag{B4}$$

where

$$\beta = \frac{\epsilon_{cr}}{2}\left(\frac{E_s A_s}{E_w A_w}\right)^2 \qquad \left(\epsilon_{cr} < e_s{}^T < \epsilon_{el}\right)$$

The thermal stress corresponding to the unit shortening of equation (B4) may be obtained from the average-stress—unit-shortening relationship and is expressed by the following relation:

$$\bar{\sigma}_s{}^T = \frac{A_w E_w}{A_s}\beta\left[\sqrt{1 + \frac{2}{\beta}\left(\alpha_s \bar{T}_s - \alpha_w \bar{T}_w\right)} - 1\right] \qquad \left(\sigma_{cr} < \bar{\sigma}_s{}^T < \sigma_{el}\right) \qquad \text{(B5)}$$

When shear stresses are present, the parabolic relation of critical stresses for combined compression and shear is used to obtain the value of ϵ_{cr} in evaluating the constant β for equations (B4) and (B5).

APPENDIX C

TESTS OF SQUARE TUBES AT ELEVATED TEMPERATURES

Six square tubes of the type described in appendix A with width-to-thickness ratios of 60 and 84 were subjected to combined compression and torsion; in addition, two opposite walls (without weld seams) were rapidly heated by two banks of quartz-tube radiators. (See ref. 3.) The other two walls were shielded from the radiators by aluminum plates which ran lengthwise of the tubes and projected diagonally outward from the corners of the tubes. Temperature distributions in the tubes of the type shown in figure 11 were obtained from thermocouple measurements, and permanent-buckling information was obtained on the tubes as described in appendix A after the tubes were unloaded and cooled to room temperature. In order to obtain measurements of the growth of permanent buckles, each tube was loaded in torsion and compression to stresses given in table 3, subjected to heat for a prescribed time, and then allowed to cool. Subsequent tests on the tube involved the same torque and compressive loads but the heating time was progressively increased. The average shear stress and compressive stress on each tube at the onset of permanent buckles is given in table 3 along with the average skin and web temperatures. The average temperatures of the skin and webs were obtained by mechanical integration of the temperature-distribution curves of the type indicated in figure 11. The average shear and compressive stresses of table 3 were converted to stresses in the heated walls on the basis of the following assumptions:

(a) The average shear stress in each wall is proportional to the shear modulus at the average temperature of the wall. (The shear modulus is assumed proportional to Young's modulus.)

(b) Buckling does not occur in the unheated walls and the normal-stress—unit-shortening relationship in the heated walls is that given by equation (1) with the exponent $1-m = \frac{1}{2}$, or

$$\bar{\sigma}_s = \sigma_e \left(\frac{\epsilon_{cr}}{e_e} \right)^{1/2} \tag{C1}$$

The resulting shear and compressive stresses are given in table 4 along with the calculations necessary to obtain the stress ratios for the onset of permanent buckles. The compressive properties of the material for various temperatures used in the calculations were obtained from

reference 8. The expansion coefficient used in the calculations is

$$\alpha = (5.4 + 0.0015T)10^{-6} \qquad (70^{\circ} F < T < 800^{\circ} F)$$

which is the equation of a straight line fitted to published data of the manufacturer of the material. The elastic limit in shear at elevated temperatures was assumed equal to the compressive elastic limit stress divided by $\sqrt{3}$ at the particular temperature.

The elementary manner in which the thermal component of compressive stress is evaluated herein presumes the simple thermal distribution shown in figure 7 rather than the actual temperature distribution indicated by figure 11. Consequently, the calculated values of thermal stress may be expected to be less accurate at the higher values of skin temperature when large thermal gradients exist and the properties of the heated skin vary considerably from the average values used in the analysis.

REFERENCES

1. Howland, W. L., and Sandorff, P. E.: Permanent Buckling Stress of Thin-Sheet Panels Under Compression. Jour. Aero. Sci., vol. 8, no. 7, May 1941, pp. 261-269.

2. Mayers, J., and Budiansky, Bernard: Analysis of Behavior of Simply Supported Flat Plates Compressed Beyond the Buckling Load Into the Plastic Range. NACA TN 3368, 1955.

3. Zender, George W., and Pride, Richard A.: The Combinations of Thermal and Load Stresses for the Onset of Permanent Buckling in Plates. NACA TN 4053, 1957.

4. Anderson, Roger A., and Anderson, Melvin S.: Correlation of Crippling Strength of Plate Structures With Material Properties. NACA TN 3600, 1956.

5. Ramberg, Walter, and Miller, James A.: Stress-Strain Relation in Shear From Twisting Test of Annulus. Res. Paper 2398, Jour. Res. of Nat. Bur. Standards, vol. 50, no. 2, Feb. 1953, pp. 125-130.

6. Kromm, A., and Marguerre, K.: Behavior of a Plate Strip Under Shear and Compressive Stresses Beyond the Buckling Limit. NACA TM 870, 1938.

7. Peters, Roger W.: Buckling of Long Square Tubes in Combined Compression and Torsion and Comparison With Flat-Plate Buckling Theories. NACA TN 3184, 1954.

8. Stein, Bland A.: Compressive Stress-Strain Properties of 17-7 PH and AM 350 Stainless-Steel Sheet at Elevated Temperatures. NACA TN 4074, 1957.

9. Stowell, Elbridge Z.: Critical Shear Stress of an Infinitely Long Plate in the Plastic Region. NACA TN 1681, 1948.

TABLE 1

EXPERIMENTAL AVERAGE STRESSES FOR THE ONSET OF PERMANENT BUCKLES AND FAILURE FOR COMPRESSION AND/OR SHEAR OF 17-7 PH (CONDITION TH 1050) STAINLESS-STEEL SQUARE TUBES AT ROOM TEMPERATURE

b/t	Onset of permanent buckles				Failure			
	$\bar{\sigma}_{pb}$, ksi	$\bar{\tau}_{pb}$, ksi	$R_{pb}{}^{C}$	$R_{pb}{}^{S}$	$\bar{\sigma}_{f}$, ksi	$\bar{\tau}_{f}$, ksi	$R_{f}{}^{C}$	$R_{f}{}^{S}$
40	75.7	0	1.00	0	89.2	0	1.00	0
	26.2	64.3	.346	.824	38.5	64.3	.432	.814
	0	78.0	0	1.00	0	79.0	0	1.00
60	52.5	0	1.00	0	68.8	0	1.00	0
	46.0	20.2	.876	.474	58.8	20.2	.855	.406
	26.2	29.1	.499	.683	42.8	29.1	.622	.584
	0	42.6	0	1.00	0	49.8	0	1.00
84	40.0	0	1.00	0	49.6	0	1.00	0
	24.4	15.2	.610	.458	38.7	15.2	.780	.390
	0	33.2	0	1.00	0	39.0	0	1.00

TABLE 2

CALCULATED VALUES OF ONSET OF PERMANENT BUCKLES FOR COMPRESSION OR SHEAR OF 17-7 PH (CONDITION TH 1050) STAINLESS-STEEL SQUARE TUBES AT ROOM TEMPERATURE

$$\left[E = 30{,}000 \text{ ksi};\ \mu = 0.3;\ \sigma_{el} = 85 \text{ ksi};\ \tau_{el} = 45 \text{ ksi};\right.$$

$$\left.\sigma_{cr} = \frac{4\pi^2 E}{12(1-\mu^2)\left(\frac{b}{t}\right)^2} = \frac{108500}{\left(\frac{b}{t}\right)^2};\ \tau_{cr} = \frac{5.34\pi^2\eta E}{12(1-\mu^2)\left(\frac{b}{t}\right)^2} = \frac{145000\eta^{a}}{\left(\frac{b}{t}\right)^2}\right]$$

b/t	σ_{cr}, ksi	τ_{cr}, ksi	$\overline{\sigma}_{pb} = \sqrt{\sigma_{cr}\sigma_{el}}$, ksi	$\overline{\tau}_{pb} = \sqrt{\tau_{cr}\tau_{el}}$, ksi
40	67.8	79.5	75.9	[b] 79.5
60	30.1	40.3	50.6	42.6
84	15.4	20.5	36.2	30.4

[a] η is the plasticity factor given in reference 9. For elastic stresses, $\eta = 1$.

[b] For critical stresses beyond the elastic limit, the stress for the onset of permanent buckles is taken equal to the critical stress.

TABLE 3

EXPERIMENTAL AVERAGE STRESSES AND TEMPERATURES FOR THE ONSET OF PERMANENT BUCKLES OF 17-7 PH (CONDITION TH 1050) STAINLESS-STEEL SQUARE TUBES SUBJECTED TO COMPRESSIVE LOAD, SHEAR, AND THERMAL STRESS

b/t	$\frac{\text{Load}}{4bt}$, ksi	$\frac{\text{Torque}}{2bt^2}$, ksi	$T_{s,pb}$, °F	$T_{w,pb}$, °F
60	0	36.2	608	114
	24.2	18.7	465	97
	36.6	19.2	455	116
84	0	14.4	600	90
	14.8	10.1	631	121
	24.2	15.0	485	90

TABLE 4

EXPERIMENTAL STRESS RATIOS FOR ONSET OF PERMANENT BUCKLES IN PLATES SUBJECTED TO COMBINED COMPRESSIVE LOAD, SHEAR, AND COMPRESSIVE THERMAL STRESS

b/t	① σ_{cr}, ksi	② τ_{cr}, ksi	③ σ_{el}, ksi	④ τ_{el}, ksi	⑤ $\sqrt{\sigma_{cr}\sigma_{el}}$, ksi	⑥ $\sqrt{\tau_{cr}\tau_{el}}$, ksi	⑦ $(\bar{\sigma}_s{}^T)_{pb}$, ksi	⑧ $(\bar{\sigma}_s{}^L)_{pb}$, ksi	⑨ $(\bar{\tau}_s)_{pb}$, ksi	$R_{pb}{}^T = \frac{⑦}{⑤}$	$R_{pb}{}^L = \frac{⑧}{⑤}$	$R_{pb}{}^S = \frac{⑨}{⑥}$
60	27.2	36.5	64.6	37.3	41.9	36.9	13.9	0	34.5	0.332	0	0.935
	28.2	37.7	71.4	41.2	44.9	39.4	27.2	12.1	18.1	.606	.269	.459
	28.9	38.7	75.6	43.7	46.7	41.1	26.2	16.9	18.8	.561	.362	.457
84	14.0	18.6	65.2	37.7	30.2	26.5	20.0	0	13.8	0.662	0	0.521
	13.9	18.5	63.4	36.6	29.6	26.0	24.5	4.2	9.6	.828	.142	.369
	14.4	19.1	70.2	40.6	31.7	27.9	16.9	6.1	14.5	.533	.192	.520

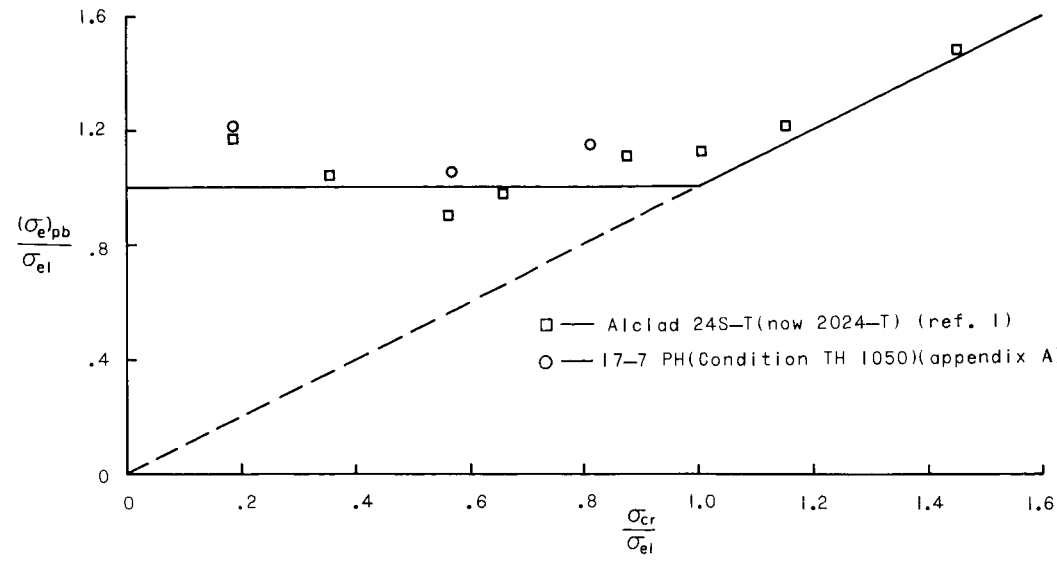

Figure 1.- Edge stress for onset of permanent buckles of plates loaded in compression.

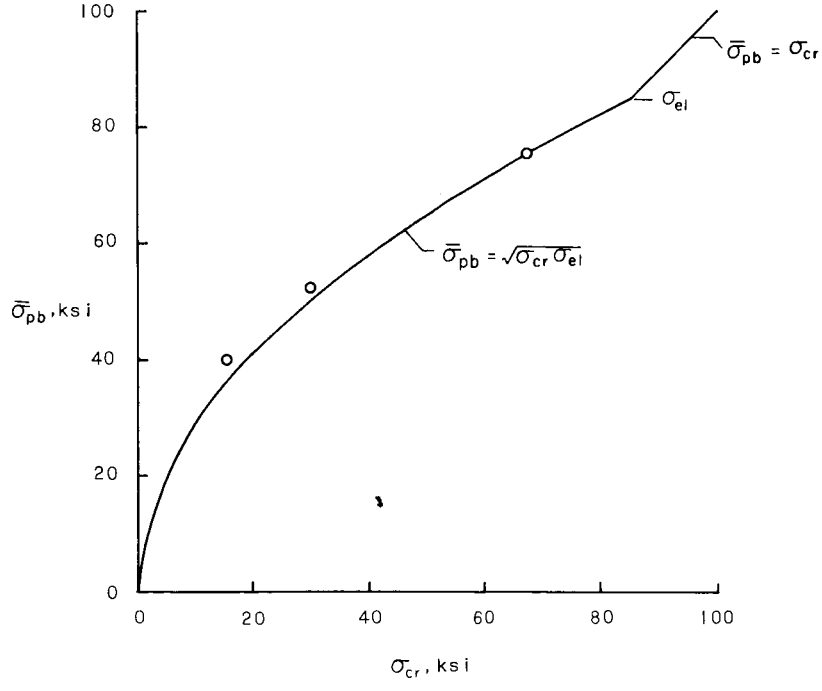

Figure 2.- Average stress for onset of permanent buckles of 17-7 PH (Condition TH 1050) stainless-steel square tubes subjected to compression.

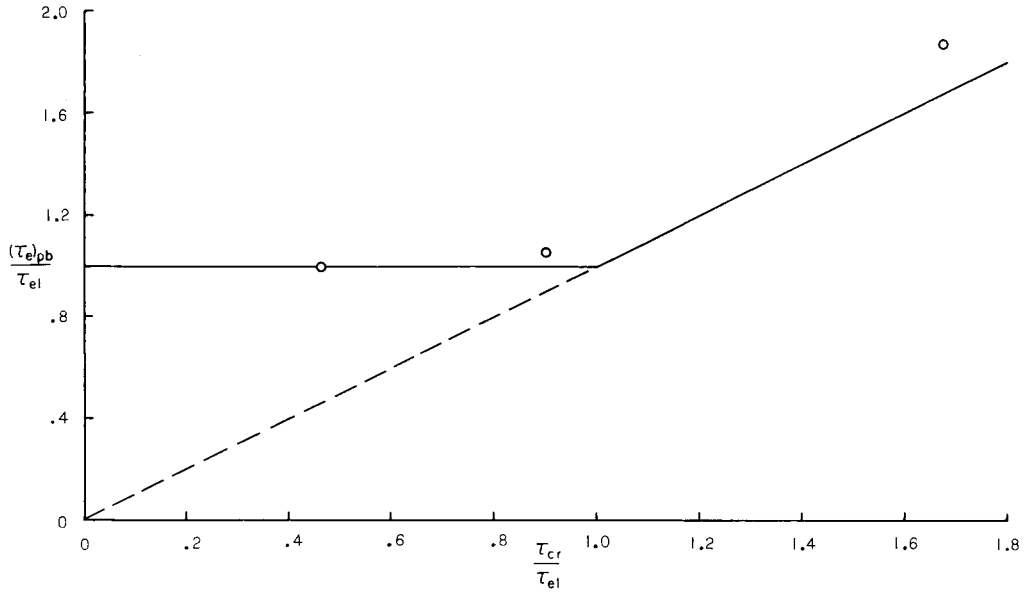

Figure 3.- Onset of permanent buckles for 17-7 PH (Condition TH 1050) stainless-steel square tubes loaded in shear.

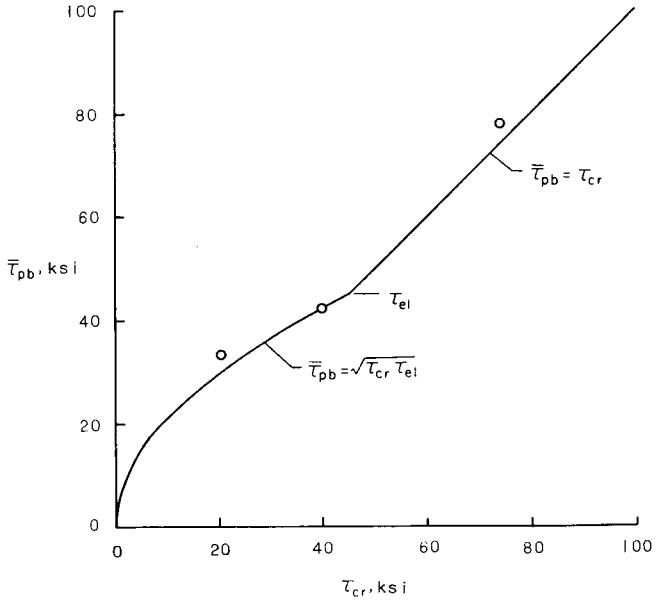

Figure 4.- Average shear stress for onset of permanent buckles of 17-7 PH (Condition TH 1050) stainless-steel square tubes subjected to torsion.

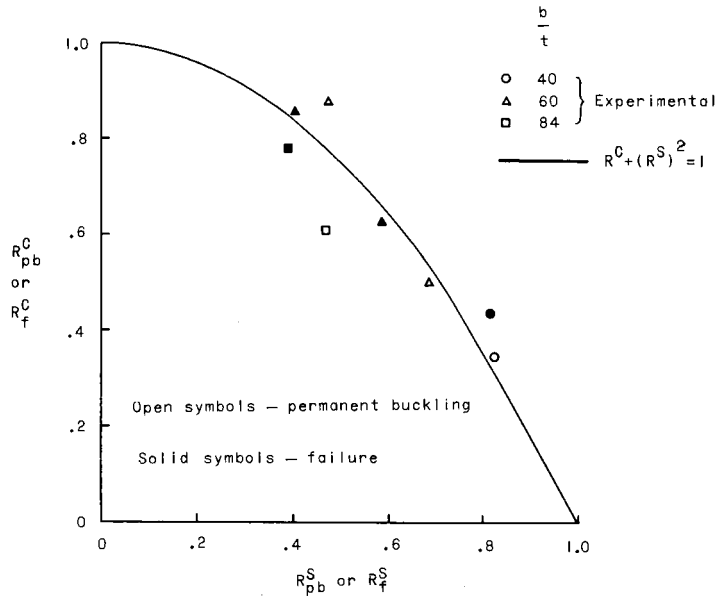

Figure 5.- Interaction curve for onset of permanent buckles and failure of 17-7 PH (Condition TH 1050) stainless-steel square tubes subjected to combined torsion and compression.

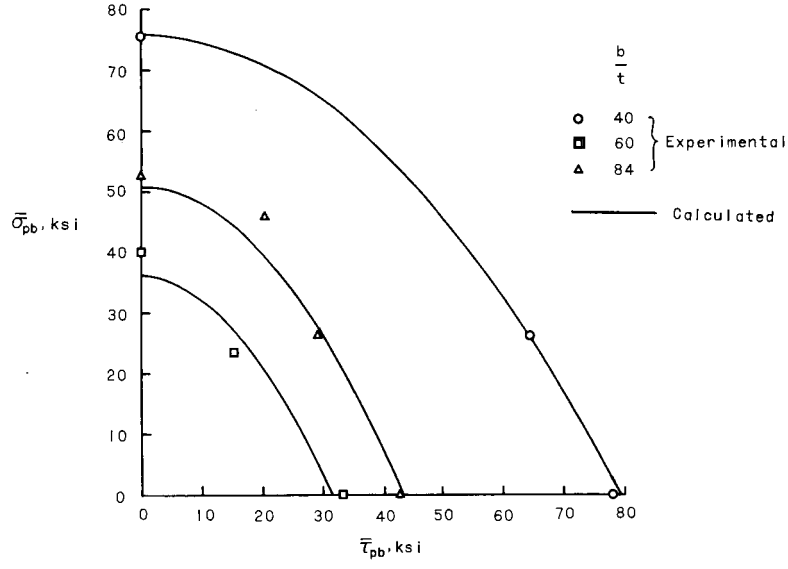

Figure 6.- Comparison of experimental and calculated stresses for onset of permanent buckles of 17-7 PH (Condition TH 1050) stainless-steel square tubes subjected to combined compression and shear.

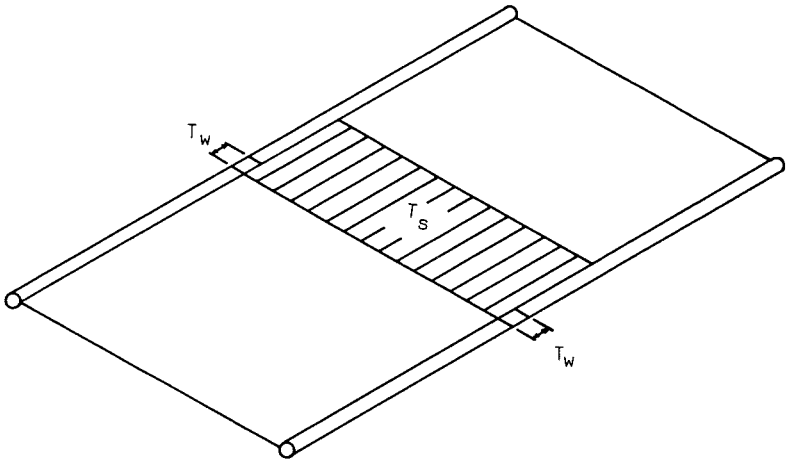

Figure 7.- Assumed temperature distribution in idealized structure used to evaluate thermal stresses.

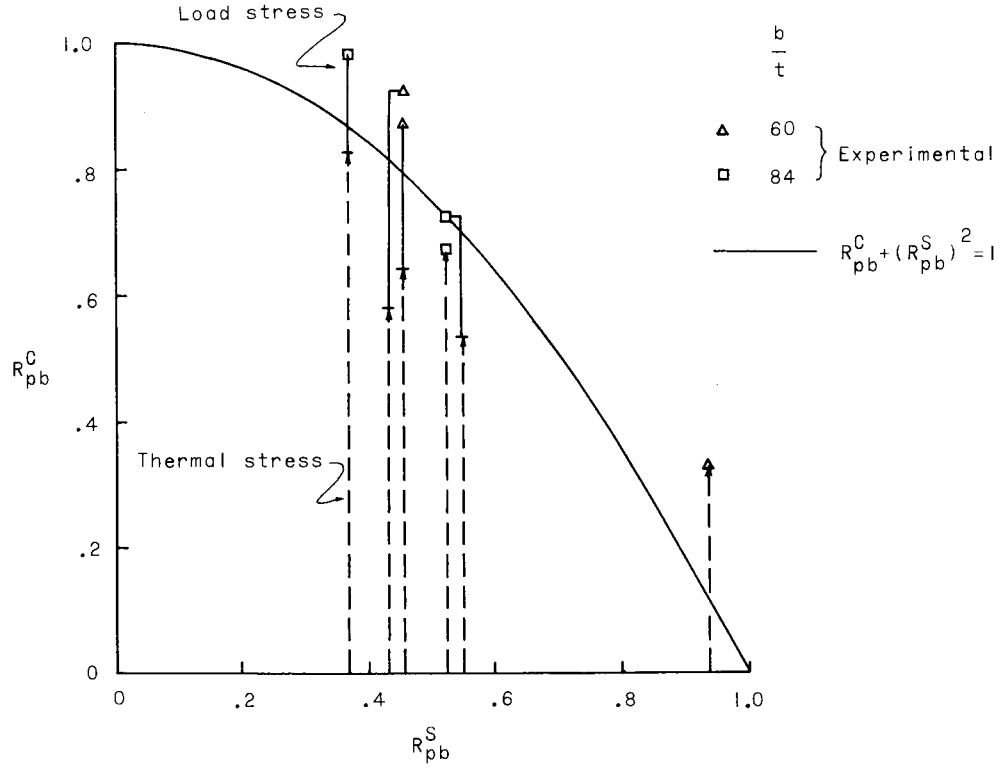

Figure 8.- Interaction curve for onset of permanent buckles of 17-7 PH (Condition TH 1050) stainless-steel square tubes subjected to shear, thermal, and compressive stresses.

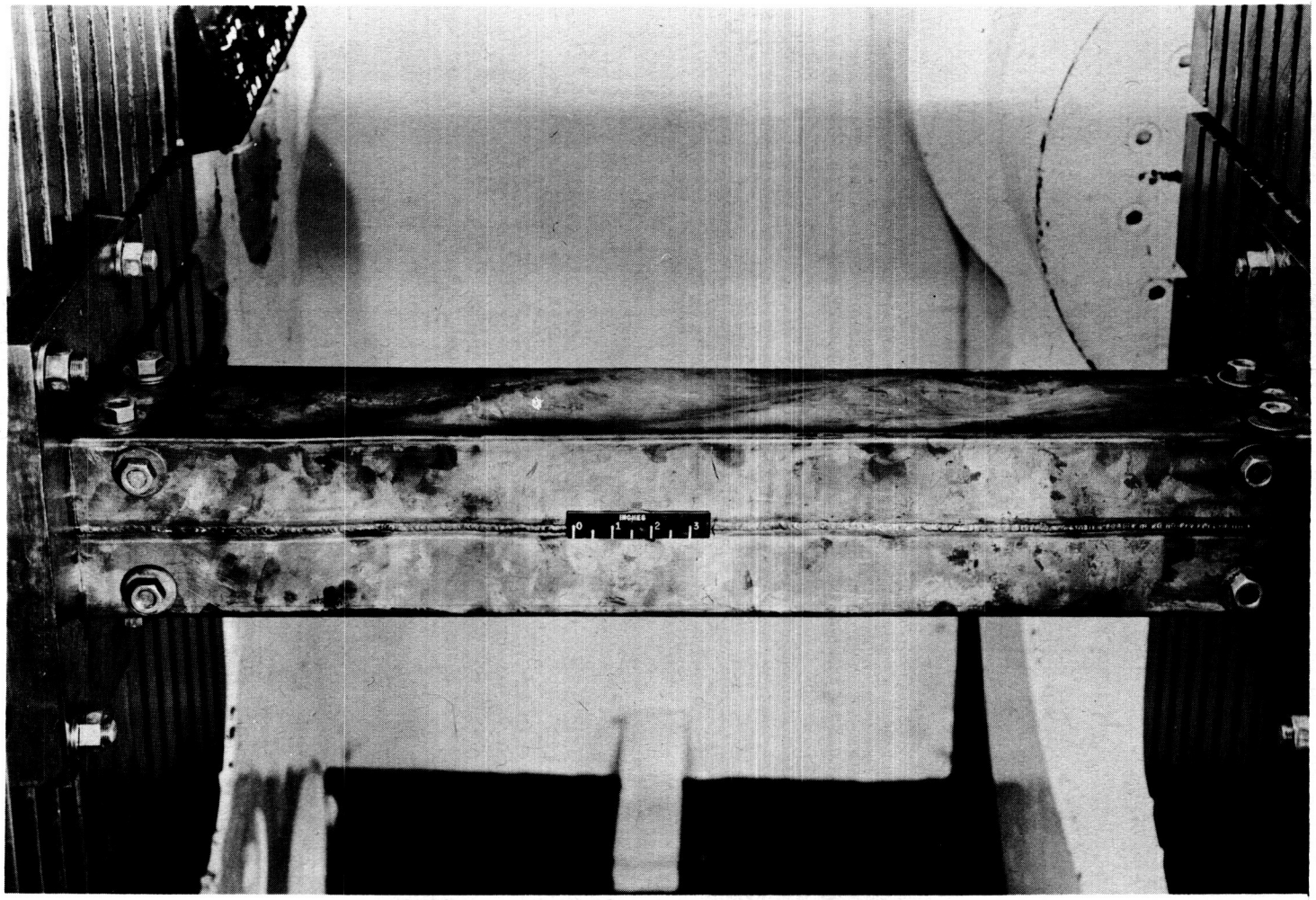

L-58-2932.1

Figure 9.- Permanent buckling of square tube subjected to combined torsion, compression, and thermal stress after unloading and cooling to room temperature. b/t = 84.

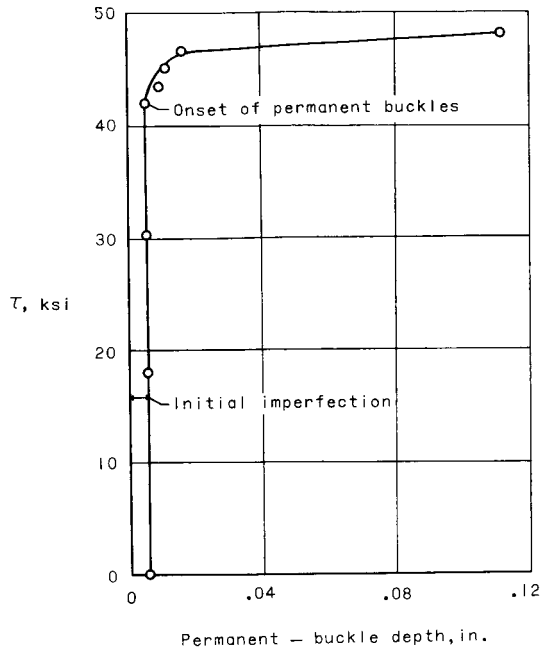

Figure 10.- Method of obtaining onset of permanent buckles. b/t = 60; 17-7 PH (Condition TH 1050) stainless-steel square tube.

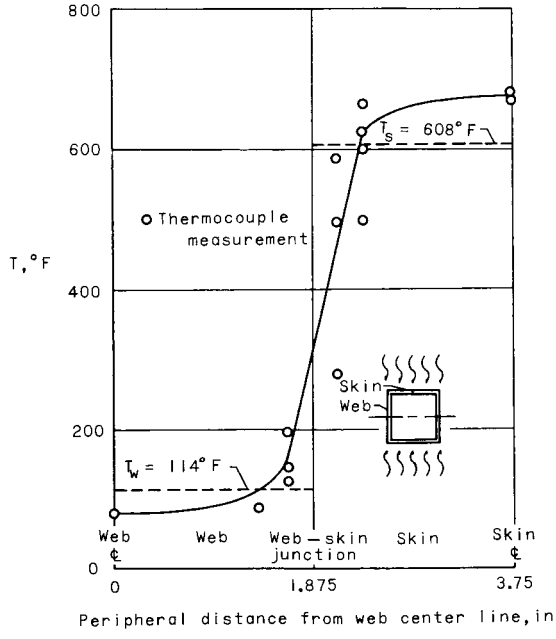

Figure 11.- Experimental temperature distribution. b/t = 60; 17-7 PH (Condition TH 1050) stainless-steel square tube.